RSC Advances

PAPER

View Article Online
View Journal | View Issue

Cite this: *RSC Adv.*, 2020, **10**, 40739

A multifunctional use of bis(methylene)bis(5-bromo-2-hydroxyl salicyloylhydrazone): from metal sensing to ambient catalysis of A3 coupling reactions†

Krisana Peewasan, *[a] Marcel P. Merkel, [b] Olaf Fuhr, [bc] Christopher E. Anson [a] and Annie K. Powell *[ab]

Received 8th September 2020
Accepted 20th October 2020

DOI: 10.1039/d0ra07687b

rsc.li/rsc-advances

The potential use of bis(methylene)bis(5-bromo-2-hydroxylsalicyloylhydrazone) as a multifunctional fluorescence sensor for Cu^{2+}, Ni^{2+}, Co^{2+} and Fe^{2+} ions was investigated. The optical behaviour shows an increase in an absorption band at 408 nm which can be ascribed to the d–d transition (UV-vis) of the metal ions and a concomitant decrease in fluorescence intensity at 507 nm. The crystallographic analysis shows the binding site of the sensor to two Cu^{2+} ions and confirms the stoichiometry of 1 : 2 (ligand to metal) which is in good agreement with a Job plot analysis. Furthermore the Cu^{2+}-complex catalyses A3 coupling reactions at 1 mol% catalytic loading; chiral propargylamine derivatives were obtained in high yield after 24 h reaction time under ambient conditions.

Introduction

The design and development of chemosensors which provide high selectivity and sensitivity towards metal ions have attracted much attention from chemists, biologists and environmental scientists.[1,2] Metal ions can play both beneficial and harmful roles depending on their speciation and concentration in natural systems. Among the 3d metal ions, the detection of these trace metals in biological systems has been intensively investigated. It is of particular interest to detect copper (Cu^{2+}) because Cu^{2+} ions are the third most abundant in the human body after Fe^{3+} and Zn^{2+}. The Cu^{2+} ions play crucial roles in several biological processes[3] such as haemopoiesis as well as various enzyme-catalysed and redox reactions.[4] Although an average concentration of Cu^{2+} in the body of 0.1 mM is required for biological processes high levels lead to various disorders such as Menkes and Wilson's diseases.[5–8] Several techniques are widely used to detect copper ions, including atomic absorption spectroscopy (AAS)[9] and inductively coupled plasma atomic emission or mass spectroscopy (ICP-AES, ICP-MS).[10] However, the biggest drawbacks of these techniques are expense, complicated sample pre-treatment procedures and high sample volumes. Thus, alternative methods which provide high selectivity, simplicity and low cost are required such as colorimetric, fluorescence and electrochemical analysis. Through targeted ligand design metallosensors with high selectivity and sensitivity can be developed. Another important requirement is to make the system low-cost and atom efficient. To this end, a number of sensors utilising fluorescent dyes both in aqueous and organic phases has been reported.[11–19] Although high selectivity and sensitivity were achieved, such fluorescent probes require meeting the challenge of multi-step synthesis and control of pH.

Copper is not only used in biological processes, but is also well known as catalyst for A3 coupling,[20–24] azide–alkyne cycloaddition (click-reaction)[25,26] and aldol-type reactions.[27] Among these, the A3 coupling reaction is of particular interest, because chiral propargylamines[28] obtained from this reaction are crucial building blocks in organic chemistry for diastereoselective and enantioselective components which exhibit biologically activities and are common in natural products.[29]

We report here the synthesis of the bis(methylene)bis(5-bromo-2-hydroxyl salicyloylhydrazone) (=$\mathbf{H_6L}$) as a new fluorescent metal chemosensor and the application of its copper complexation for catalysis. $\mathbf{H_6L}$ was designed as a potentially decadentate ligand with coordination of ten oxygen or nitrogen donor atoms. The decadentate coordination sites are provided by oxygen and nitrogen atoms arranged suitably for complexation to transition metal ions. Furthermore, the

[a]*Institute of Inorganic Chemistry, Karlsruhe Institute of Technology, Engesserstrasse 15, 76131 Karlsruhe, Germany. E-mail: krisana.peewasan@kit.edu; annie.powell@kit.edu*

[b]*Institute of Nanotechnology, Karlsruhe Institute of Technology Campus North, Hermann-von-Helmholtz-Platz 1, 76344 Eggenstein-Leopoldshafen, Karlsruhe, Germany*

[c]*Karlsruhe Nano Micro Facility Karlsruhe Institute of Technolog, Hermann-von-Helmholtz-Platz 1, 76344 Eggenstein-Leopoldshafen, Germany*

† Electronic supplementary information (ESI) available: Experimental section, X-ray structure determinations, NMR spectra, IR spectra, UV-vis spectra and CIFs of complexes. CCDC 2001537. For ESI and crystallographic data in CIF or other electronic format see DOI: 10.1039/d0ra07687b

salicyloylhydrazone groups introduced in this ligand system can provide fluorescence properties making it possible track optical behaviour for various coordination compounds in comparison with those for the free ligand. The selectivity and sensitivity towards the metal dications Cu^{2+}, Pb^{2+}, Cd^{2+}, Zn^{2+}, Ni^{2+}, Co^{2+}, Fe^{2+} and Sn^{2+} in DMSO solution were investigated. Crystallographic analysis of the Cu^{2+}-complex reveals the nature of the complexation of the **H_6L** sensor showing a ligand : metal stoichiometry of 1 : 2. The $[Cu_2(H_5L)(NO_3)_2]NO_3\cdot 0.5H_2O\cdot 2CH_3CN$-complex was also used in a catalytic study for the A3 coupling reaction with 1 mol% loading under ambient conditions.

Experimental

Materials and method

All reagents and solvents were used as received from commercial suppliers without further purification. Infrared spectra were recorded on a PerkinElmer Spectrum GX FT-IR spectrometer in ATR mode in the range 4000–400 cm^{-1}. The following abbreviations were used to describe the peak characteristics: br = broad, sh = shoulder, s = strong, m = medium and w = weak. NMR spectra of the compounds were measured using a Bruker Ultrashield plus 500 (500 MHz) and Varian 500 MHz spectrometer. ^{1}H- and ^{13}C-measurements were recorded using deuterated solvents and referenced to tetramethylsilane (TMS) as an internal standard (δ = 0 ppm). The single crystal X-ray diffraction (SCXRD) data were collected on a STADIVARI diffractometer using Ga-Kα, λ = 1.34143 Å radiation with area detection using a Dectris Eiger2 R 4M detector. Powder X-ray diffraction (PXRD) measurements were performed on a STOE STADI-P diffractometer with Cu-Kα radiation. The optical properties were investigated using Fluoromax-4 spectrofluorometer and Shimadzu UV-24500 in the range 200–800 nm at room temperature using 1 cm path length cells. The stock solution of **H_6L** (100 μM) and the corresponding metal ions solutions (1000 μM) were prepared in DMSO.

Spectral analysis

The UV-vis absorption and fluorescence experiments were performed in DMSO. The spectral titration experiments were accomplished through a stepwise addition of Cu^{2+} solution (100 μM) to a solution of **H_6L** (25 μM) in DMSO. The absorption intensity was recorded in the range 200–800 nm reference to DMSO. The fluorescence intensity was recorded at $\lambda_{ex}/\lambda_{em}$ = 310 nm/507 nm after shaking the solution and allowing to stand for 5 min to ensure proper mixing. Both the excitation and emission slits were set to 10.0 nm. The stoichiometry of the complex formed between **H_6L** and Cu^{2+} was determined by preparing a series of solutions of **H_6L** and Cu^{2+} at ratios of 1 : 9, 2 : 8, 3 : 7, 4 : 6, 5 : 5, 6 : 4, 7 : 3, 8 : 2, and 9 : 1 and recording the absorbance. The plot of [HG] *versus* [H]/([H] + [G]) was drawn to determine the stoichiometry using a Job plot analysis.

Preparation of the ligand (H_6L)

A mixture of 5-bromosalicylaldehyde (**1**, 4.20 g, 20 mmol), *N*,*N*″-dimethylethylenediamine (**2**, 0.88 g, 10 mmol) and paraformaldehyde (1.2 g) was refluxed in ethanol for 16 h. The corresponding intermediate (**3**) was obtained in 68% yield after purification using column chromatography. It was then reacted with 2-hydroxybenzhydrazide (**4**, 3.48 g, 13.5 mmol) under reflux in ethanol (100 mL) for 16 h. The product bis(methylene) bis(5-bromo-2-hydroxyl salicyloylhydrazone) (**H_6L**) was obtained as a yellow solid (92% yield) after removal of ethanol and washing with Et_2O.

Preparation of the copper complex $[Cu_2(H_5L)(NO_3)_2]NO_3\cdot 0.5H_2O\cdot 2CH_3CN$

H_6L (78 mg, 0.1 mmol) was dissolved in 5 mL of a mixture of acetonitrile and methanol (1 : 1, % v/v) at room temperature. Then $Cu(NO_3)_2\cdot 2.5H_2O$ (56 mg, 2.0 mmol) was added to the solution and the reaction mixture was stirred at room temperature for 30 min. After standing for 7 days, crystals were collected by filtration (70% yield based on the ligand **H_6L**). The powder product was characterised using IR, and PXRD (see ESI†).

Results and discussion

Design and synthesis of H_6L and its optical properties

Ligand **H_6L** was designed to have ten possible coordination sites from both O and N atoms as well as the potential to exhibit strong fluorescence. The preparation of **H_6L** is versatile and straightforward, providing the final product in excellent (92%) yield *via* a two step reaction (Scheme 1).

The optical properties of **H_6L** were investigated. A 25 μM stock solution of **H_6L** (100 μM) in DMSO was prepared for use as a working solution for a Job plot analysis and fluorescence experiments. The absorption maxima of the bands were found

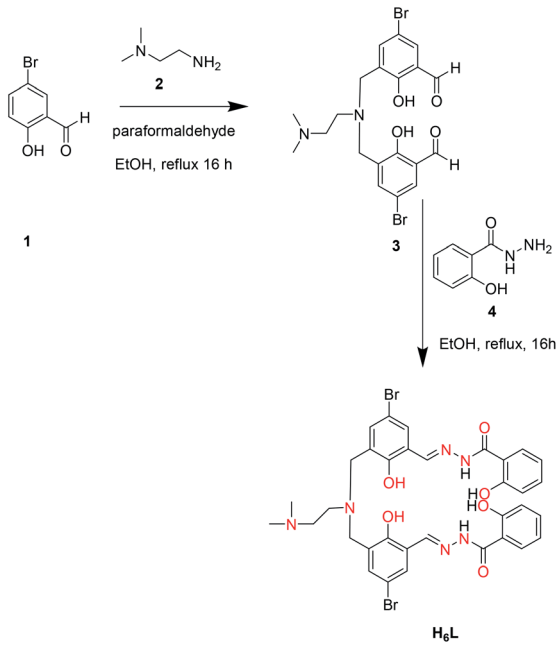

Scheme 1 Synthetic route to the ligand H_6L.

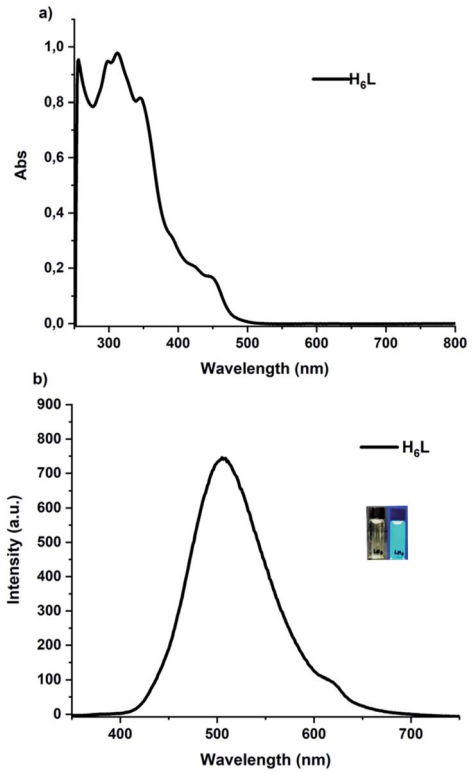

Fig. 1 (a) Absorption and (b) fluorescence spectra of H_6L. The measurement was carried out at room temperature, 25 μM in DMSO and λ_{ex} = 310 nm, slit; 10 nm/10 nm were used.

at 296 nm, 310 nm, 345 nm and 450 nm, the latter of which can be attributed to the n → π* transition of the C=N moiety. The absorption maximum at 310 nm was selected as excitation wavelength for the fluorescence experiment and both the excitation and emission slits were set to 10 nm. Strong fluorescence intensity of the free ligand **H_6L** at 507 nm was observed (Fig. 1).

Use of H_6L for Cu^{2+} sensing

The potential use of **H_6L** to detect Cu^{2+} ion was investigated by titration of a 25 μM solution of **H_6L** with a 100 μM solution of Cu^{2+} in DMSO. A decrease in intensity of the absorption at 346 nm and an increase in intensity of a new band at 408 nm were observed on increasing the number of equivalents of Cu^{2+}. The band at 408 nm is attributed to a d–d transition. Corresponding fluorescence titration experiments of the sensor **H_6L** with increasing equivalents of Cu^{2+} show a concomitant decrease in fluorescence intensity at 507 nm of **H_6L**. The fluorescence intensity of the free sensor **H_6L** was completely quenched when 2.0 equivalents of Cu^{2+} were added. A Job plot analysis established a 1 : 2 stoichiometry of **H_6L** to Cu^{2+} (Fig. 2) with the lower limit of detection (LOD) found to be 0.036 μM, calculated using the UV-vis absorption data.

Chemoselectivity of H_6L towards M^{2+}

The response of **H_6L** towards other M^{2+} ions was investigated. Absorptions were observed in the 370–450 nm range (Fig. 3a),

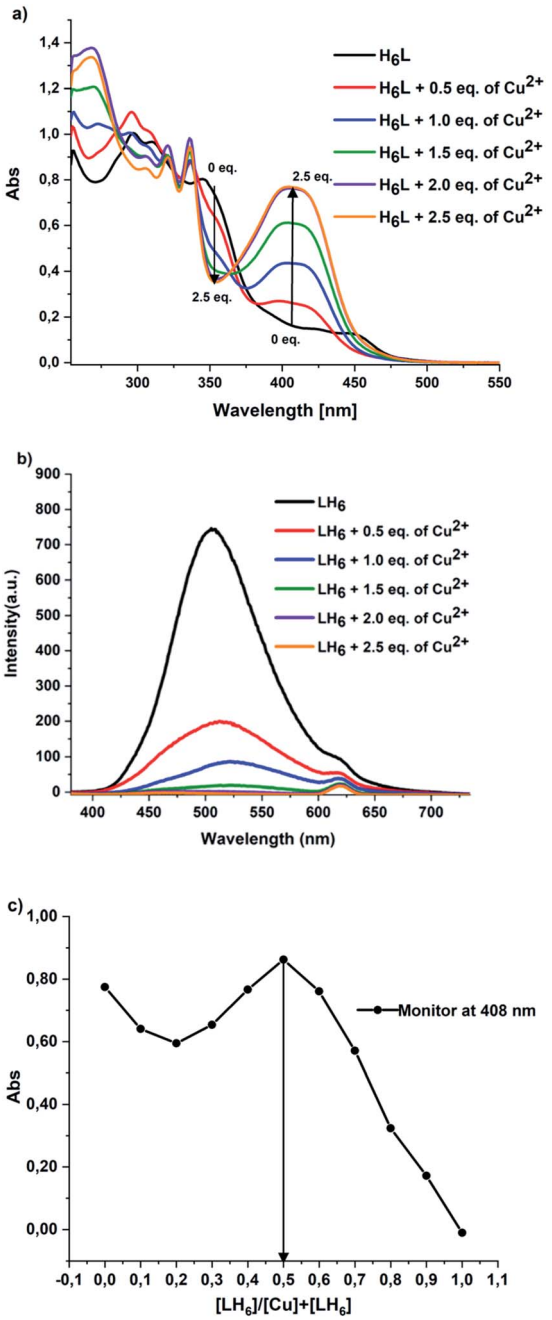

Fig. 2 (a) UV-vis titration spectra, (b) fluorescence titration spectra (λ_{ex} = 310 nm, slit; 10 nm/10 nm) of H_6L (25 μM) with increasing amount of Cu^{2+} in DMSO and (c) Job plot showing a 1 : 2 ratio of H_6L to Cu^{2+} ions.

but these were much weaker than the absorption at 408 nm observed for Cu^{2+} ions. The intensities of these absorptions show the trend $Cu^{2+} > Ni^{2+} > Co^{2+} > Zn^{2+} > Sn^{2+} > Fe^{2+} > Pb^{2+} > Cd^{2+}$.

The fluorescence behaviour of the **H_6L** + M^{2+} systems showed similar trends to those of the absorption spectra. The fluorescence intensity decreases according to $Cu^{2+} > Ni^{2+} > Co^{2+} > Fe^{2+} \ggg Sn^{2+} \gg Zn^{2+} \gg Pb^{2+} \gg Cd^{2+}$ (Fig. 3b) with a dramatic

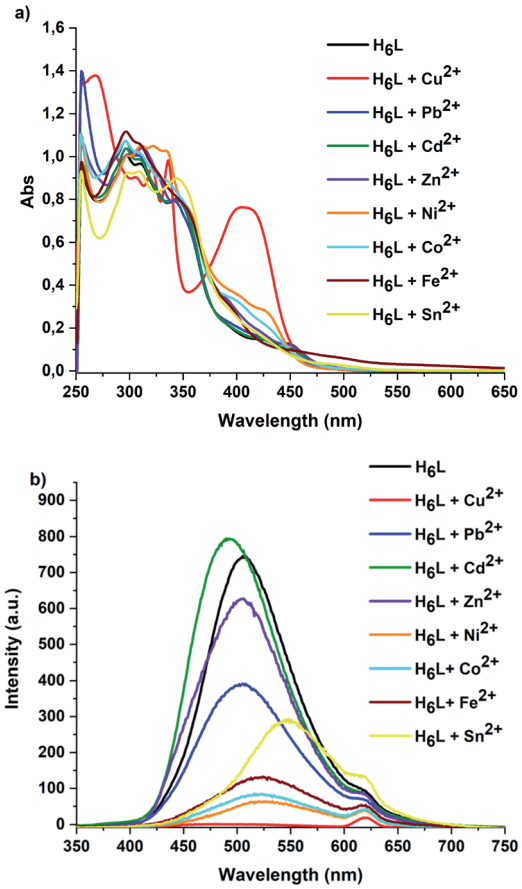

Fig. 3 (a) UV-vis spectra of H_6L + M^{2+}, (b) fluorescence spectra of H_6L + M^{2+} (λ_{ex} = 310 nm, slit; 10 nm/10 nm) of H_6L (25 μM) and M^{2+} (25 μM) in DMSO.

break between Fe^{2+} and Sn^{2+}. Thus Cu^{2+}, Ni^{2+}, Co^{2+} and Fe^{2+} are the best candidates for chemosensing with **H_6L**.

Structural details for $[Cu_2(H_5L)(NO_3)_2]NO_3\cdot 0.5H_2O\cdot 2CH_3CN$

Fig. 4 shows the structural features of $[Cu_2(H_5L)(NO_3)_2]NO_3\cdot 0.5H_2O\cdot 2CH_3CN$. The coordination sphere of Cu(1) consists of two-coordinating O atoms from the ligand (O(2) and O(3)), one nitrogen atom of the ligand (N(2)), one bridging O atom from one nitrate (O(7)) and one coordinated O atom from another nitrate (O(10)). The coordination environment of Cu(2) consists of two O atoms from the ligand (O(4) and O(5)), one nitrogen atom from the ligand (N(5)) and one bridging O atom from nitrate (O(7)), thus Cu(1) and Cu(2) are bridged *via* O(7), whereas O(10A) only coordinates to Cu(1). Furthermore, N(4) of the ligand is protonated and a N(4)–H···O(13) intermolecular hydrogen bond to a nitrate anion is build. O(5) and O(2) form either intermolecular hydrogen bonds to a water molecule. The protonated N(3) atom of the ligand form intramolecular hydrogen bonds to O(3) and O(4). Likewise, N(1) and N(6) build hydrogen bonds to O(1) and O(6), respectively. The Cu–O distance ranges from 1.889(2) to 2.595(4) Å, whereas the Cu–N distance is between 1.910(3) and 1.931(3) Å. The Cu–Cu distance is 3.5612(7) Å and the angle between Cu–O(7)–Cu is 126.62(15).

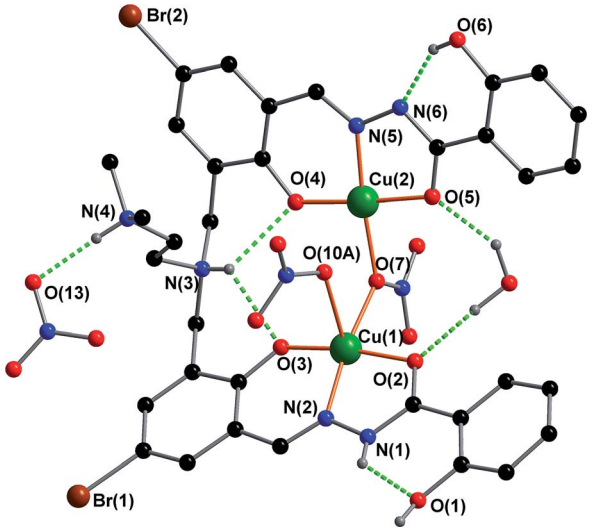

Fig. 4 The structure of $[Cu_2(H_5L)(NO_3)_2]NO_3\cdot 0.5H_2O\cdot 2CH_3CN$. Colour codes: green (Cu), blue (N), red (O), black (C) and brown (Br). The hydrogen bonds are shown as green dashed line. Solvent molecules (MeCN) in the lattice and H atoms which are not involved in hydrogen bonds are omitted for clarity.

Table 1 Optimisation reaction of A3 coupling reaction

Entry	Catalytic loading	Conversion yield (%)
1	5 mol%	95[a]
2	**1 mol%**	**92**[a]
3	0.5 mol%	80[a]
4	0.1 mol%	78[a]
5	**1 mol%**	**95**[b]

[a] Conversion yields were calculated by the integration of ^{1}H NMR at 9.60 ppm and 3.50 ppm after 16 h reaction time. [b] The comparison of entry 2 and entry 5 at 1 mol% loading performed over 16 h under the same reaction conditions performed 24 h, respectively, is shown in bold.

The positive charges of the two Cu^{2+} ions are balanced by the deprotonated ligand at N(6) and three nitrate anions and the SHAPE[30] analysis shows that the best coordination geometry of Cu(1) is spherical square pyramid with a deviation value 2.463 and the Cu(2) is appear square planar with a deviation value 0.246 but has O(10B) making long contact with 2.582 Å. The square-pyramidal coordination sphere of Cu(1) consists of one N and two O atoms from the ligand (N(2), O(2) and O(3)) and one unidentate bridging O atom O(7) from one nitrate, with a further O atom O(10) from the other nitrate in the apical position. The coordination environment of Cu(2) is similar to Cu(1) although Cu(2)-O(10A) is rather longer at 2.595(4) Å, and the molecule has approximate mirror symmetry. One of the hydrazine groups (N(1)) is still protonated, while N(6) is deprotonated and together with the three nitrates balances the charge. N(4) of the ligand is protonated with N(4)–H···O(13) forming an intermolecular hydrogen bond to a nitrate anion. The Cu–O distance ranges from 1.889(2) to 2.595(4) Å, whereas the Cu–N distance is between 1.910(3) and 1.931(3) Å. O(7)

Table 2 Extended scope of A3 coupling reaction catalysed by $[Cu_2(H_5L)(NO_3)_2]NO_3\cdot 0.5H_2O\cdot 2CH_3CN$

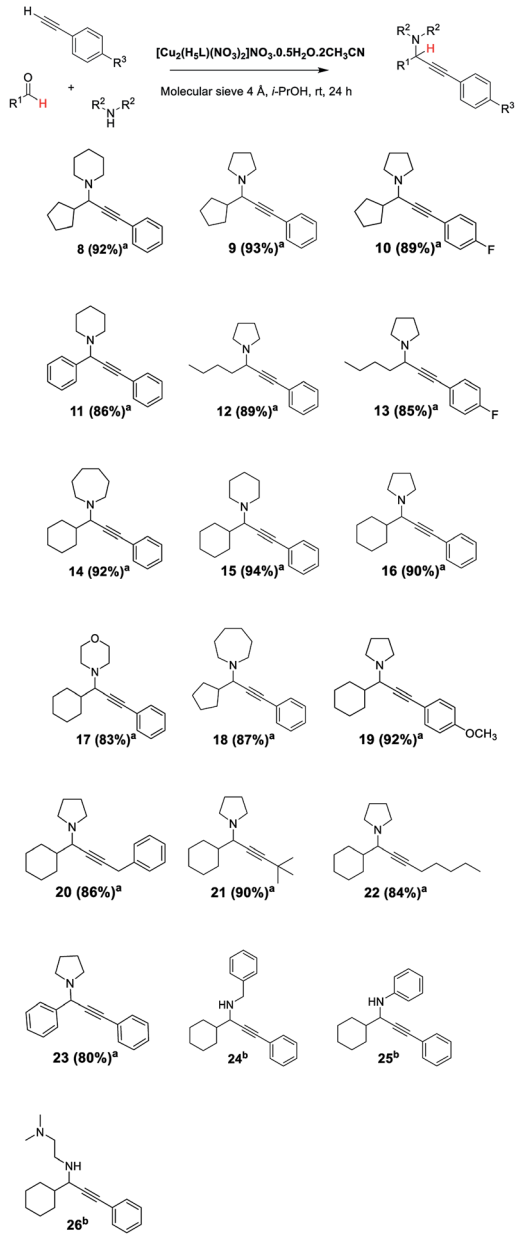

[a] Reaction conditions: 1 mol% catalytic loading, 2.0 mmol aldehyde, 2.2 mmol amine and 2.4 mmol alkyne, 4 Å molecular sieves, solvent *i*-PrOH, room temperature for 24 h. [b] No products obtained.

forms a unidentate eq,eq-bridge with Cu(1)–O(7)–Cu(2) = 126.62(15)° and Cu(1)···Cu(2) = 3.5612(7) Å. The other nitrate ligand shows minor disorder between unidentate bridging (78%) and syn,syn-bridging (22%) modes. SHAPE[30] analysis shows that the best coordination geometry of Cu(1) is spherical square pyramid with a deviation value 2.463, while Cu(2) is square planar with a deviation value 0.246, although with a long contact of 2.582 Å to O(10B). A summary of the crystallographic refinement data (Table S1†) and SHAPE analysis (Table S2†) are given in the ESI.†

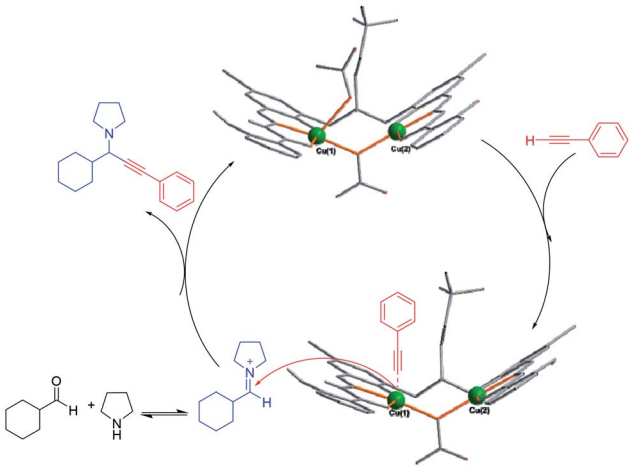

Fig. 5 Possible mechanism for the A3 coupling reaction catalysed by $[Cu_2(H_5L)(NO_3)_2]NO_3\cdot 0.5H_2O\cdot 2CH_3CN$.

Catalytic study

The investigation of the potential of $[Cu_2(H_5L)(NO_3)_2]NO_3\cdot 0.5H_2O\cdot 2CH_3CN$ as a catalyst for the A3 coupling reaction was explored. Cyclopentane carboxaldehyde (**5**), piperidine (**6**) and phenylacetylene (**7**) were chosen as reagents for a model reaction. The catalytic loading was first investigated with the reaction performed under aerobic conditions at room temperature for 16 h (Table 1). The efficiency of this catalytic system can be followed by monitoring the disappearance of the aldehyde proton signal at 9.60 ppm and the appearance of a new peak of the quaternary proton of the propargylamine product at 3.50 ppm.

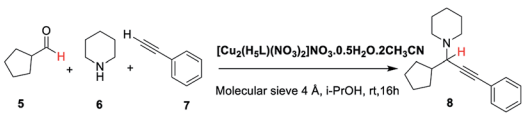

The results show that with 5 mol% catalytic loading the maximum conversion yield was obtained (95%, entry 1). However, reducing the catalytic loading to 1 mol% only affects the conversion yield by 3%. Increasing the reaction time to 24 h raises the conversion yield to 95% (entry 5). Thus, the catalytic loading of 1 mol% and reaction time of 24 h were chosen as test conditions for this system. The scope of the catalytic system was investigated using various aldehydes, alkynes and amines (Table 2). The reactions were carried out at room temperature for 24 h in *i*-PrOH and 4 Å molecular sieves were used to trap water. After 24 h, the reaction mixture was filtered through celite and washed with dichloromethane. The crude products were purified using column chromatography.

The high efficiency catalysis is clearly seen for the various combinations of aldehyde and secondary amine, with products attained in high yield with low catalytic loading, short reaction time and mild reaction conditions.[31–34] However, no products were obtained when the aromatic and/or aliphatic primary amines were used. In addition, the stability of the catalyst used in this reaction was investigated using ESI-TOF mass

spectrometry. The $[Cu_2(H_5L)(NO_3)_2]NO_3 \cdot 0.5H_2O \cdot 2CH_3CN$ was dissolved in *i*-PrOH and the change in mass was monitored after 24 h, 48 h and 72 h (Fig. S27†). Regarding the results from mass spectroscopy, in solution, one coordinated nitrate was found to be removed from Cu(1) of the coordination cluster (mass cal. = 969.9178 *m*/*z*, found = 969.9068 *m*/*z*, Fig. S27†) resulting in a free reactive site on copper. This allows a possible mechanism for the A3 coupling reaction of this system to be proposed (Fig. 5). Furthermore, the compound was tested as a catalyst for click chemistry but without any success.

Conclusion

Bis(methylene)bis(5-bromo-2-hydroxyl salicyloylhydrazone) can be used as a multiple functionality ligand. Coordination complexes formed with this ligand can be used as a highly selective and sensitive fluorescent sensor for Cu^{2+}, Ni^{2+}, Co^{2+} and Fe^{2+} ions. The molecular structure of the copper(II) complex confirms the binding mode of the ligand with the metal to ligand stoichiometry of 2 : 1 in line with results from a Job plot analysis. The presence of a d–d band at 408 nm proves that the copper is in the 2+ state. In addition, the application of the $[Cu_2(H_5L)(NO_3)_2]NO_3 \cdot 0.5H_2O \cdot 2CH_3CN$ for catalysing A3 coupling reactions was found to have high efficiency in providing a wide range of products in high yields (>80%) with catalytic loading of 1 mol% and 24 h reaction time. Moreover, the stability of the catalytic system has been investigated and the results show the catalyst is stable over 72 h in *i*-PrOH solution. Furthermore, we extended the scope of this catalytic system for copper catalysed azide–alkyne cycloaddition (CuAAC) using benzyl azide and phenyl acetylene as a model reagent. However, the expected triazole product was not obtained. This can be explained by the fact that the Cu^{2+} is not usually suitable for click chemistry.

Conflicts of interest

The authors declare no conflict of interest.

Acknowledgements

We thank the DFG for funding through SFB/TRR 88 "3MET" and the Helmholtz Association *via* POF STN. We would like to thank Prof. Dr Dieter Fenske for collecting the crystallographic data.

References

1 D. T. Quang and J. S. Kim, *Chem. Rev.*, 2010, **110**, 6280–6301.
2 B. Kaur, N. Kaur and S. Kumar, *Coord. Chem. Rev.*, 2018, **358**, 13–69.
3 M. Uauy, R. Olivares and M. Gonzalez, *Am. J. Clin. Nutr.*, 1998, **67**, 952S–959S.
4 H. Tapiero, D. M. Townsend and K. D. Tew, *Biomed. Pharmacother.*, 2003, **57**, 386–398.
5 D. J. Waggoner, T. B. Bartnikas and J. D. Gitlin, *Neurobiol. Dis.*, 1999, **6**, 221–230.
6 C. Vulpe, B. Levinson, S. Whitney and J. Gitschier, *Nat. Genet.*, 1993, **3**, 7–13.
7 K. J. Barnham, C. L. Masters and A. I. Bush, *Nat. Rev. Drug Discovery*, 2004, **3**, 205–214.
8 I. Scheinberg and I. H. Sternlieb, *Am. J. Clin. Nutr.*, 1996, **63**, 842S–845S.
9 A. P. S. Gonzáles, M. A. Firmino, C. S. Nomura, F. R. P. Rocha, P. V. Oliveira and I. Gaubeur, *Anal. Chim. Acta*, 2009, **636**, 198–204.
10 Y. Liu, P. Liang and L. Guo, *Talanta*, 2005, **68**, 25–30.
11 Y. Zhou, J. Zhang, H. Zhou, Q. Zhang, T. Ma and J. Niu, *J. Lumin.*, 2012, **132**, 1837–1841.
12 D. Zhang, Y. Ma and R. An, *Res. Chem. Intermed.*, 2015, **41**, 5059–5069.
13 X. Cheng, Y. Zhou, Y. Fang, Q. Rui and C. Yao, *RSC Adv.*, 2015, **5**, 19465–19469.
14 Y. Hu, J. Zhang, Y. Z. Lv, X. H. Huang and S. L. Hu, *Spectrochim. Acta, Part A*, 2016, **157**, 164–169.
15 F. A. Abebe and E. Sinn, *Tetrahedron Lett.*, 2011, **52**, 5234–5237.
16 Y. S. Mi, Z. Cao, Y. T. Chen, Q. F. Xie, Y. Y. Xu, Y. F. Luo, J. J. Shi and J. N. Xiang, *Analyst*, 2013, **138**, 5274–5280.
17 S. Prabhu, S. Saravanamoorthy, M. Ashok and S. Velmathi, *J. Lumin.*, 2012, **132**, 979–986.
18 U. Fegade, S. K. Sahoo, S. Attarde, N. Singh and A. Kuwar, *Sens. Actuators, B*, 2014, **202**, 924–928.
19 H. Yu, J. Y. Lee, S. Angupillai, S. Wang, S. Feng, S. Matsumoto and Y. A. Son, *Spectrochim. Acta, Part A*, 2015, **151**, 48–55.
20 V. A. Peshkov, O. P. Pereshivko and E. V. Van Der Eycken, *Chem. Soc. Rev.*, 2012, **41**, 3790–3807.
21 C.-J. L. Woo-Jin Yoo and L. Zhao, *Aldrichimica Acta*, 2011, **2**, 43–51.
22 C. Wei, Z. Li and C. J. Li, *Synlett*, 2004, **9**, 1472–1483.
23 L. Zani and C. Bolm, *Chem. Commun.*, 2006, **41**, 4263–4275.
24 I. Jesin and G. C. Nandi, *Eur. J. Org. Chem.*, 2019, **16**, 2704–2720.
25 H. C. Kolb, M. G. Finn and K. B. Sharpless, *Angew. Chem., Int. Ed.*, 2001, **40**, 2004–2021.
26 C. W. Tornøe, C. Christensen and M. Meldal, *J. Org. Chem.*, 2002, **67**, 3057–3064.
27 Z. Liu, Z. Zhang, G. Zhu, Y. Zhou, L. Yang, W. Gao, L. Tong and B. Tang, *Org. Lett.*, 2019, **21**, 7324–7328.
28 D. Castagnolo, N. Scalacci, A Toscani and K Lauder, *Chem. Rev.*, 2017, **117**, 14091–14200.
29 B. V. Rokade, J. Barker and P. J. Guiry, *Chem. Soc. Rev.*, 2019, **48**, 4766–4790.
30 M. Llunell, D. Casanova, J. Cirera and S. Alvarez, SHAPE version 2.1, Universitat de Barcelona, Barcelona, 2013.
31 C. Wei, Z. Li and C. J. Li, *Org. Lett.*, 2003, **5**, 4473–4475.
32 L. Shi, Y. Q. Tu, M. Wang, F. M. Zhang and C. A. Fan, *Org. Lett.*, 2004, **6**, 1001–1003.
33 Y. Zhang, P. Li, M. Wang and L. Wang, *J. Org. Chem.*, 2009, **74**, 4364–4367.
34 E. Loukopoulos, M. Kallitsakis, N. Tsoureas, A. Abdul-Sada, N. F. Chilton, I. N. Lykakis and G. E. Kostakis, *Inorg. Chem.*, 2017, **56**, 4898–4910.